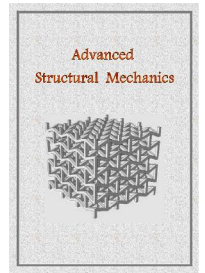


Advanced Structural Mechanics

journal homepage: <http://asm.sku.ac.ir>



Investigating the effect of coating thickness on detection of large-diameter pipe coating disbondment using guided Lamb waves

Pourya Rafieinia^a, Amin Yaghootian^{a,*}, Ali Valipour^a, Vahid Khoshkharesh^b

^aMechanical Engineering Department, Faculty of Engineering, Shahid Chamran University of Ahvaz, Golestan Blvd, Ahvaz (postcode: 61357-83151), Iran

^bKhuzestan gas company, Shahid Bandar Square - the beginning of Bandar Imam Khomeini Highway, Ahvaz (postcode: 6174799755), Iran

Article received: 2022/04/05, Article revised: 2022/09/14, Article accepted: 2022/11/07

ABSTRACT

Coated pipes are used in corrosive conditions such as water and soil. This paper presents an effective method to study the effect of coating thickness on detection of pipe coating disbondment. In this regard, finite element modelling of ultrasonic guided Lamb wave propagation is conducted to study this defect. In order to simulate guided wave propagation in a pipe, a two-dimensional model can be employed as it is used for plates when the thickness-to-radius ratio of the pipe is less than 0.1. Therefore, the two-dimensional finite element modelling of the epoxy-coated steel pipe has been conducted in this paper. The second mode of the Lamb wave (m_2) in the bilayer plate has been generated at a suitable frequency. In order to model the pipe coating disbondment, a specified condition is applied in the place of disbonding. Signals reflected from the disbondment are received by a sensor. Reflections and many mode conversions seen at the beginning and end of the disbonding result in disbonding detection. Coating thickness affects the probability of detection of this defect.

Keywords: Disbonding; Guided Lamb wave; Coated pipe; Two dimensional finite element modelling; Thickness

1. Introduction

Pipelines are installed in various industries to transport gas, oil, water, and other products. When the pipeline is in a corrosive environment (such as buried pipes), the condition can cause pipe corrosion (which is one of the serious problems in the oil and gas industries). One of the effective methods to protect the oil and gas pipelines is to apply coatings to them. The common materials used as a coating in pipeline industries are epoxy and bitumen [1]. Unfortunately, the disbonding defect may appear during manufacturing or operation due to various reasons.

* Corresponding author at: Mechanical Engineering Department, Faculty of Engineering, Shahid Chamran University of Ahvaz, Ahvaz, Iran

E-mail address: a.yaghootian@scu.ac.ir

DOI: 10.22034/asm.2022.13810.1002: http://asm.sku.ac.ir/article_11344.html

Disbonding of pipe coating can cause serious damages such as corrosion to the pipe, reduction of pipe lifetime, and fluid leakage. The disbondings are sub-surface damages, which are not detected through visual inspection and ultrasonic non-destructive testing (NDT) methods have thus been used to inspect the structures [2]. The ultrasonic non-destructive testing is based on the propagation of ultrasonic waves. These waves can be divided into two general categories: bulk waves and guided waves. Guided waves have low attenuation during the propagation so that a long distance along the structures can be inspected from a single transducer position. Therefore, it is particularly attractive for use on buried pipes [3]. In fact, in this technique, there is no need for point-to-point inspection, which is usually common in the inspection by bulk waves, resulting in significant time and cost saving. However, in this technique, it is difficult to interpret the signals due to the guided wave dispersion and propagation of a large number of modes. Accordingly, understanding the propagation of these waves and inspection by them via simulation seems to be necessary.

Guided waves in pipes can be divided into two general categories. The first group propagates in a circumferential direction which includes circumferential Lamb type (CLT) waves and circumferential shear horizontal (CSH) waves. The second group of the guided waves propagates in axial direction, including longitudinal and torsional waves with both axisymmetric and non-axisymmetric modes. The main advantage of guided waves in the axial direction is the long-range inspection capability compared to the circumferential guided wave whose propagation is limited to circumferential geometry [4]. Therefore, guided waves in the axial direction are used in this study. Previous studies have shown that when the thickness-to-radius ratio of the pipe is less than 0.1, a two-dimensional model can be employed to simulate guided wave propagation in a pipe as it is used for plates [1]. The reason is because in this situation, the effect of pipe curvature on guided waves is negligible. For example, propagation of axisymmetric longitudinal wave modes in pipes becomes equal to propagation of Lamb waves in plates and dispersion curves and wave structures of them will be the same as each other [5]. After removing all torsional modes and non-axisymmetric longitudinal modes in pipes and consequently pure excitation of axisymmetric longitudinal modes under certain conditions, a two-dimensional plate model (Lamb waves) can be employed instead of the pipe model. The two-dimensional plate model can be a good demonstration of how these waves propagate and significantly reduce the computational run-time. Luo et al. [6] showed that a plate model often gives a quick and sufficient solution for a large-diameter pipe. Bingham and Hinders [7] used a plate model to mimic the guided waves in a large-diameter pipe sample. Li and Rose [8] used plate approximation to calculate phase velocity and determine the angular profile of waves propagating in a large-diameter pipe. Gaul et al. [9] used dispersion curve of plate model to locate cracks in a pipe with high diameter to thickness ratio.

2. Literature review

Since the entire thickness of a material can be interrogated using a variety of Lamb wave modes, Lamb waves can detect not only surface damage but internal damage as well [10]. Other advantages of this type of waves include fast inspection and low cost [11]. According to the mentioned Lamb wave properties, researchers have employed them to detect damages such as notches, cracks, etc. [12, 13]. In the earliest studies on Lamb waves, ultrasonic probes were used, but recently, piezoelectric sensors, such as lead zirconate titanate (PZT), are preferred due to their low weight, low cost, small size, and good mechanical coupling with the plate [14]. Alkassar et al. [12] used PZT wafers as actuators and sensors to transmit and receive Lamb waves, respectively.

In the present paper, axisymmetric disbonding of large-diameter pipe coating is evaluated using guided waves. Therefore, this paper focuses on the propagation of Lamb waves in bilayer plates and the obtained results are valid for both large-diameter pipes (pipes with a thickness-to-radius ratio less than 0.1) and plates. Therefore, the two-dimensional finite element modelling of Lamb waves in a plate with the mentioned defect is used based on the ABAQUS/Explicit. Then the second Lamb wave interaction with the disbonding is studied.

3. Materials and methods

A plate model can be an effective solution for large-diameter pipes. The excitation in a free plate will generate guided Lamb waves. Lamb waves are composed of transverse and longitudinal waves and include various modes all of which are dispersive. In fact, their velocities are a function of frequency [15]. Since in bilayer plates, the geometry

of the structure is not symmetric about the mid-plane, there are not any symmetric or anti-symmetric modes. Therefore, Lamb wave modes are defined by m_n where n indicates the mode number. The number of existing Lamb wave modes goes up as the frequency increases. Since the existence of many Lamb wave modes makes the analysis difficult, an appropriate frequency must be chosen to prevent generating high-order modes (higher than m_2). To model the propagation of Lamb waves, a two-dimensional finite element modelling has been used in which a 4-node plane strain element (CPE4R) has been chosen for a 6.5 meters long epoxy/steel plate. Dynamic modelling has been conducted based on the ABAQUS/Explicit. The properties and thickness of the material are shown in Table 1 [16]. A schematic of the finite element modelling is shown in Fig. 1.

Lamb waves have been excited by piezoelectrics. Instead of electro-mechanical coupled field simulations for PZT actuators and sensors, a point-force model has been used. Instead of modelling PZT elements, their mechanical effect (point-forces) is modeled. Point-force model is a beneficial tool for the Lamb waves behavior analysis [17]. The bottom layer is steel and the top layer (coating) is epoxy. Considering the complete bonding between the coating and the plate, a constraint should be applied between them so that all the points of the coating and the plate are bonded together, and when one point of the plate vibrates, the adjacent point in the coating vibrates as well. In this paper, the constraint "tie" is used to bond the coating and the plate together. Using this constraint at the interface of two layers makes the displacement of the points of the two layers that are bonded together equal to each other with no relative motion in between. In fact, the constraint "tie" creates a complete bonding. In order to model disbonding, tie constraint is applied at the interface of epoxy and steel except for the disbonding region. This type of disbonding modelling does not change the volume of the layers and it is in accordance with the real disbonding. Because of the m_1 mode generation in addition to m_2 mode and their difference in velocity (i.e. m_1 velocity is lower than m_2 velocity), the long plate (6.5 meters) is modeled to study the behavior of m_2 individually. In finite element simulations, the layers of the bilayer plate are modeled individually and their properties are assigned. In order to receive signals generated by PZT actuators (i.e. forces exerted at single points at the left of the structures) and study the disbonding, sensor A is located at 38 cm before the beginning of disbonding. Sensor A is chosen to be far from the excitation (4.422 meters) to prevent the echo of m_1 mode appearing in signals captured by sensor A. The length of disbonding is 40 cm (long disbonding) and consequently, distinguishing the extra echoes (explained in section 4) that are appeared in signals captured by sensor A will be easier. The excitation pulse is the pulse that is usually used in the simulation of ultrasonic waves and is shown in Fig. 2.

The excitation pulse is consisted of three cycles with a central frequency of 0.05 MHz (Fig. 2) and is given by Eq. (1):

$$F(t) = \begin{cases} \left[1 - \cos\left(\frac{2\pi ft}{N}\right)\right] \cos(2\pi ft) & 0 \leq t \leq \frac{N}{f} \\ 0 & \text{otherwise} \end{cases} \quad (1)$$

where f is the central frequency, N is the number of cycles and t is time.

In order to guarantee convergent solutions in time domain and adequately accurate solutions in spatial domain during wave propagation simulations, two important criteria must be pointed out [16]:

- The maximum length of each element (Δl_{\max}) should be smaller than a tenth of the smallest wavelength (λ_{\min}), i.e.

Table 1. Geometry and properties of material [16].

Material	Density (kg/m^3)	Transversal wave velocity (km/s)	Longitudinal wave velocity (km/s)	Thickness (mm)
Steel	7800	3.19	5.9	4
Epoxy E&C 2057	1600	1.45	2.96	3

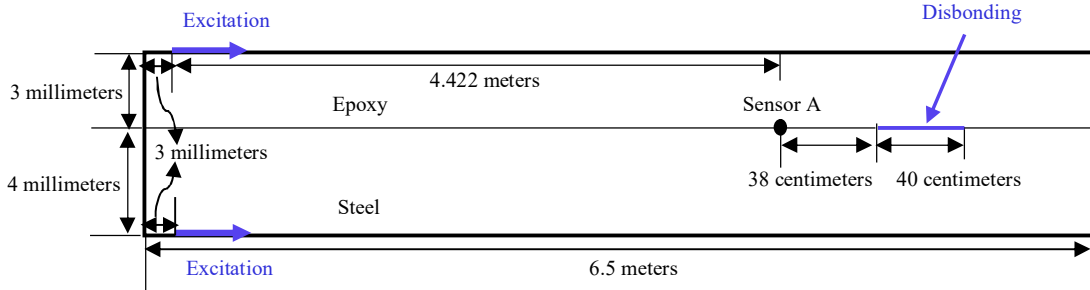


Fig. 1. Schematic of finite element modelling of bilayer plate.

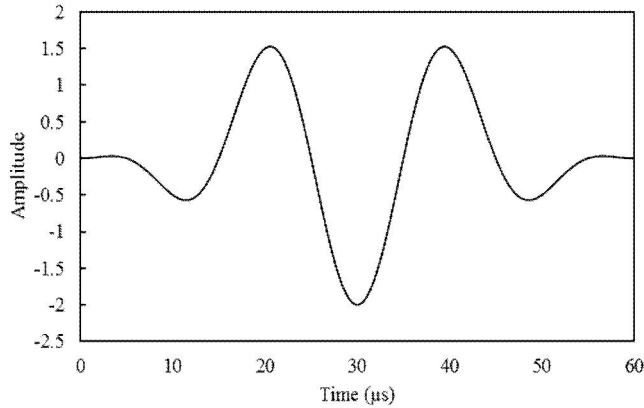


Fig. 2. Form of the excitation pulse in 0.05 MHz.

$$\Delta l_{\max} \leq \frac{\lambda_{\min}}{10} \tag{2}$$

- The integration time step (Δt) has to be selected according to the smallest element length (Δl_{\min}) and fastest wave velocity that exists in the problem (c_{\max}), i.e.

$$\Delta t < \frac{\Delta l_{\min}}{c_{\max}} \tag{3}$$

For finite element simulation, the phase velocities of m_1 and m_2 modes at 0.05 MHz are first calculated by dispersion curve of steel/epoxy bilayer plate. Then the minimum wavelength will be determined and the maximum dimension of elements can be obtained according to the first criterion. In this frequency, the minimum phase velocity is 2302 m/s, and the minimum wavelength is 0.04604 m. Therefore, Δl_{\max} is smaller than 0.004640. Moreover, as the maximum phase velocity is 5280 m/s in this frequency, the integration time step should be smaller than 0.198 μ s according to the second criterion if the smallest element length is 0.001 meter. The Meshed model of the structure in ABAQUS is shown in Fig. 3.

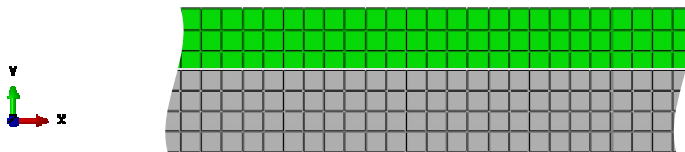


Fig. 3. Meshed model of steel plate coated with epoxy layer in ABAQUS.

The element size is 0.001 in Fig. 3. In this figure, the color of the bottom layer (steel) is different from the color of the top layer (epoxy). In the finite element model, the group velocities of Lamb wave modes (m_1 and m_2) are determined. These velocities have a good agreement with the group velocity dispersion curve obtained analytically with MATLAB code (Fig. 4). In fact, in Fig. 4 the group velocities of m_1 and m_2 modes in 0.05 MHz are 2303 and 4992.3 m/s, respectively. The corresponding velocities in the finite element method are 2341.3 and 5021.2 m/s, respectively. These results demonstrate the effectiveness and validity of the proposed finite element method.

4. Result and discussion

In order to indicate the effect of disbonding presence and interaction of m_2 mode with it, time-history of displacement magnitude at sensor A is shown in Fig. 5. Additionally, this displacement is plotted for the defect-free structure. According to Fig. 5, the presence of disbonding leads to the extra echoes generation. In fact, these echoes are generated due to mode conversions and reflections in the disbonding region. Coating (epoxy layer) thickness can affect amplitudes of these extra echoes. For instance, the effect of this parameter (i.e. coating thickness) on the amplitude of the echo located in the red square in Fig. 5 will be examined below. Reflection coefficient of the mentioned echo (ratio of maximum amplitude of this echo to maximum amplitude of incident m_2) is 0.0667. In fact, the maximum amplitude of incident m_2 and maximum amplitude of this echo are 10.58 and 0.70655 pm, respectively. After reducing the coating thickness, decreasing or increasing in the amplitude of this echo is checked. Reflection coefficients for different coating thicknesses at a constant frequency (0.05 MHz) are calculated in Table 2.

As shown in Table 2, the reflection coefficient decreases as coating thickness decreases. It means that the thinner the coating, the smaller the amplitudes of the extra echoes. Consequently, when the incident mode is m_2 , excessive reduction of coating thickness makes it difficult to detect disbonding. As the extra echoes cannot be well observed in thin coatings, the effect of frequency has also been checked. In this regard, the central frequency of the excitation pulse is changed while the dimensions of the bilayer plate are considered to be constant. The results show that when frequency increases, amplitudes of the extra echoes decrease and vice versa. Therefore, it is suggested to reduce the frequency when pipe coating is thin (it consequently becomes difficult to observe the extra echoes and to detect disbonding).

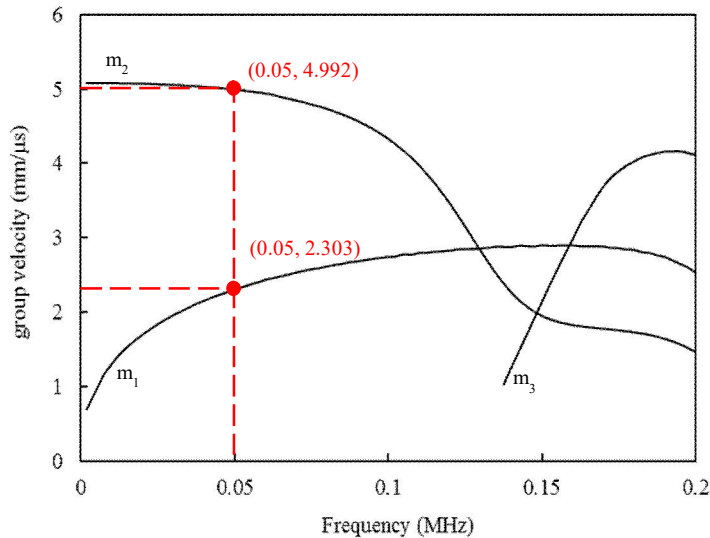


Fig. 4. Group velocity dispersion curve of a steel plate of 4 mm thickness coated with 3 mm epoxy.

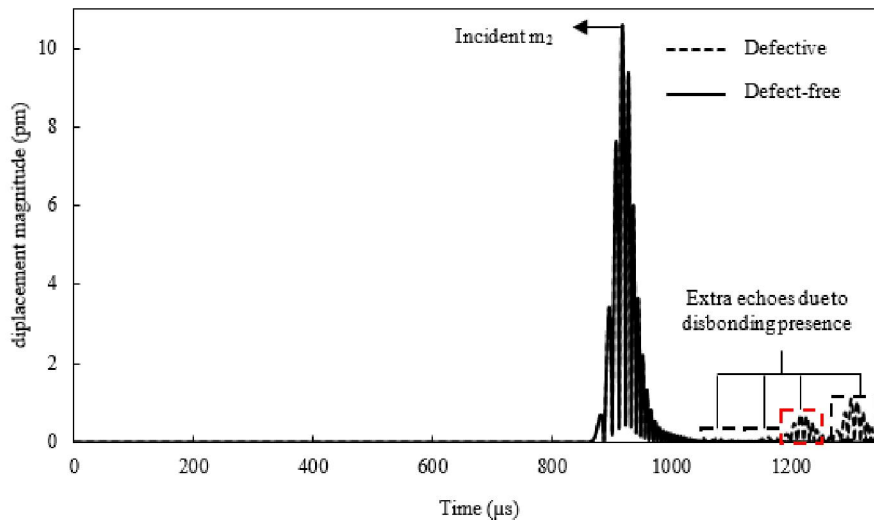


Fig. 5. Time-histories of displacement magnitude at sensor A for defective and defect-free bilayer plate.

Table 2. The effect of coating thickness on amplitude of echo located in red square in Fig. 5.

Coating thickness (mm)	Maximum amplitude of incident m_2 (pm)	Maximum amplitude of the mentioned echo (pm)	Reflection coefficient
3	10.58	0.70655	0.0667
2.5	11.3401	0.6674	0.0588
2	11.1218	0.5201	0.0463

5. Conclusions

Because of the wide application of coated pipes, this paper studies the effect of coating thickness on disbonding detection by guided Lamb waves. At first, finite element modelling and important criteria to model wave propagation by finite element method were pointed out. The accuracy of the proposed finite element method was then verified according to the consistency of the velocities of m_1 and m_2 in the finite element modelling with corresponding velocities in the analytical dispersion curve. In order to prevent the excitation of modes whose order is higher than m_2 , the excitation frequency was considered less than the cutoff frequency of m_3 . When the Lamb wave passes the disbonding region, it generates extra echoes in the time-history of displacement magnitude at sensor A. Consequently, the disbonding was detected based on the differences between defective and defect-free time-histories. The effect of coating thickness on amplitudes of generated echoes and possibility of disbonding detection was studied. Results show that the thinner the coating, the smaller the amplitudes of the extra echoes at a constant frequency for m_2 .

Acknowledgment

The authors are grateful to the Research Council of Shahid Chamran University of Ahvaz for its financial support (GN 96/3/02/16670).

References

- [1] Hua, J., Rose, J.L., 2010. Guided wave inspection penetration power in viscoelastic coated pipes. *Insight-Non-Destructive Testing and Condition Monitoring*. 52(4), 195-205.
- [2] Ramadas, C., Balasubramaniam, K., Joshi, M., Krishnamurthy, C. V., 2009. Interaction of the primary anti-symmetric Lamb mode (A_0) with symmetric delaminations: numerical and experimental studies. *Smart Materials and Structures*. 18(8), 085011.
- [3] Khalili, P., Cawley, P., 2016. Excitation of single-mode Lamb waves at high-frequency-thickness products. *IEEE transactions on ultrasonics, ferroelectrics, and frequency control*. 63(2), 303-312.
- [4] Luo, W., 2005. Ultrasonic guided waves and wave scattering in viscoelastic coated hollow cylinders. PhD thesis, The Pennsylvania State University.
- [5] Davies, J., 2008. Inspection of pipes using low frequency focused guided waves. PhD thesis, University of London.
- [6] Luo, W., Zhao, X., Rose, J. L., 2005. A guided wave plate experiment for a pipe. *Journal of pressure vessel technology*. 127(3), 345-350.
- [7] Bingham, J., Hinders, M., 2009. Lamb Wave Detection of Delaminations in Large Diameter Pipe Coatings. *the Open Acoustics Journal*. 2, 75-86.
- [8] Li, J., Rose, J.L., 2006. Natural beam focusing of non-axisymmetric guided waves in large-diameter pipes. *Ultrasonics*. 44(1), 35-45.
- [9] Gaul, T., Schubert, L., Weihnacht, B., Frankenstein, B., 2014. Localization of defects in pipes using guided waves and synthetic aperture focussing technique (SAFT). *EWSHM-7th European Workshop on Structural Health Monitoring*.
- [10] Li, W., Xu, C., Cho, Y., 2016. Characterization of Degradation Progressive in Composite Laminates Subjected to Thermal Fatigue and Moisture Diffusion by Lamb Waves. *Sensors*. 16(2), 260.
- [11] Zeng, L., Lin, J., Huang, L., 2017. A Modified Lamb Wave Time-Reversal Method for Health Monitoring of Composite Structures. *Sensors*. 17(5), 955.
- [12] Alkassar, Y., Agarwal, V.K., Alshrihi, E., 2017. Simulation of Lamb Wave Modes Conversions in a Thin Plate for Damage Detection. *Procedia Engineering*. 173, 948-955.
- [13] ZHAO, Y., Li, F., Cao, P., Liu, Y., Zhang, J., Fu, S., Zhang, J., Hu, N., 2017. Generation mechanism of nonlinear ultrasonic Lamb waves in thin plates with randomly distributed micro-cracks. *Ultrasonics*. 79, 60-67.
- [14] Feng, B., Ribeiro, A.L., Ramos, H.G., 2018. Interaction of Lamb waves with the edges of a delamination in CFRP composites and a reference-free localization method for delamination. *Measurement*. 122, 424-31.
- [15] Rose, J.L., 2014. *Ultrasonic guided waves in solid media*. Cambridge University Press.
- [16] Mu, J., 2008. Guided Wave Propagation and Focusing in Viscoelastic Multi-layered Hollow Cylinders. PhD thesis, Engineering Mechanics, The Pennsylvania State University.
- [17] Nienwenhui, J.H., Neumann, J.J., Greve, D.W., Oppenheim, I.J., 2005. Generation and Detection of Guided Waves Using PZT Wafer Transducers. *IEEE transactions on ultrasonics, ferroelectrics, and frequency control*. 52(11), 2103-11.